

Case 1

Michael Owston, DVM, MS, DACVP; Eui Jae Sung DVM, MS, PHD, DACVP

Slide: 15 99M

Signalment: Cynomolgus Macaque, male, approximately 18 months old, Vietnam origin

History: This animal tested positive for Plasmodium by serology during a pre-study health check. It was treated with a standard anti-malarial protocol (0.5 ml/kg of 62.5/25 mg/ml Atovaquone/Proguanil for three days) and was found dead on the fourth day (the day after the last dose).

Clinical pathology findings: On the blood smear, few erythrocytes contain intracellular parasites that vary in size from 1-2 um ring forms to larger trophozoites or probable gametocyte stage organisms that fully occupy the erythrocyte. The cytoplasm of the parasites stains light blue and often contains small, 1 um or less, black or golden-brown, anisotropic pigment granules (hemozoin or malaria pigment).

There were no other abnormalities in the clinical chemistry or hematology exam.

Gross findings: There were no gross findings noted.

Microscopic findings:

Spleen: The red pulp was diffusely expanded (congestion) and contained abundant brown-black pigment granules (approximately 1-2 microns), which was sometimes within cells in larger clumps (macrophages).

Liver: Brown-black pigment granules were noted within Kupffer cells and within macrophages (often several macrophages were in clusters) within the sinusoids.

Lung: Several bronchi, bronchioles, and adjacent alveoli had necrotic epithelium, walls, and septa, with abundant hemorrhage, fibrin, and some neutrophils, with the occasional presence of refractile (foreign) material.

Trachea: The epithelium was extensively eroded and necrotic, and there were many neutrophils within the lumen and infiltrating the propria-submucosa.

Diagnosis:

Spleen: Congestion; pigment

Liver: Pigment, macrophages

Lung: Inflammation, necrotizing, neutrophilic, with hemorrhage and foreign material

Trachea: Inflammation, necrotizing, neutrophilic

Discussion:

Splenic congestion and brown-black pigment accumulation within the spleen and liver were consistent with hemozoin pigment from Plasmodium infection.

Necrotizing inflammation in the lung with foreign material and inflammation in the trachea were consistent with aspiration pneumonia. This was considered the cause of death in the animal. The reason for aspiration in the animal may be secondary to vomiting, which could have been due to either the malarial disease, or a reaction to the treatment drugs.

Hemozoin is a product of hemoglobin (heme) digestion by the parasites. The substance has been implicated in anemia, cytokine dysfunction, and immunosuppression in hosts, and also is important for the parasite itself, and so has been a target of antimalarial drug research (Ihekwereme et al.)

Because of transport of cynomolgus macaques from areas where malaria is endemic, animals are routinely screened for infection. Most animals will respond to a standard 3-day treatment of Atovaquone/Proguanil (commonly used in humans to prevent and treat malaria). Failure to treat infected animals could lead to clinical disease, and even death (Ohta et al.), though most animals will recover naturally (Peterson et al.). Infection by one or multiple strains of *Plasmodium spp.* can be particularly high in some areas (Yusuf et al.) In a retrospective study of 800 cynomolgus monkeys from endemic areas that were used in toxicity studies, hemozoin deposition was noted within 29-84% of animals depending upon the origin (Ohta et al.). Therefore, when conducting studies from animals originating in these areas, it is important to distinguish hemozoin pigment from test article-induced pigment accumulation if there appears to be a dose-responsive effect. Also, because malarial disease can affect the conduct of the study, pre-screening of animals from endemic areas could be considered to reduce potential confounders when conducting a study (Sharma et al).

References:

Ihekwereme CP, Esimone CO, Nwanegbo EC. Hemozoin inhibition and control of clinical malaria. *Adv Pharmacol Sci.* 2014;2014:984150. doi: 10.1155/2014/984150. Epub 2014 Feb 9. PMID: 24669217

Ohta E, Nagayama Y, Koyama N, Kakiuchi D, Hosokawa S. Malaria in cynomolgus monkeys used in toxicity studies in Japan. *J Toxicol Pathol.* 2016 Jan;29(1):31-8. doi: 10.1293/tox.2015-0051. Epub 2015 Nov 20. PMID: 26989299

Sharma D, Priest H, Wilcox A. Pseudoreticulocytosis by the ADVIA 2120 Hematology Analyzer and Other Hematologic Changes in a Cynomolgus Macaque (*Macaca fascicularis*) With Malaria. *Toxicol Pathol.* 2022 Jul;50(5):684-692. doi: 10.1177/01926233221083217. Epub 2022 Mar 14. PMID: 35285348

Peterson MS, Joyner CJ, Brady JA, Wood JS, Cabrera-Mora M, Saney CL, Fonseca LL, Cheng WT, Jiang J, Lapp SA, Soderberg SR, Nural MV, Humphrey JC, Hankus A, Machiah D, Karpuzoglu E, DeBarry JD; MaHPIC-Consortium; Tirouvanziam R, Kissinger JC, Moreno A, Gumber S, Voit EO, Gutiérrez JB, Cordy RJ, Galinski MR. Clinical recovery of *Macaca fascicularis* infected with *Plasmodium knowlesi*. *Malar J.* 2021 Dec 30;20(1):486. doi: 10.1186/s12936-021-03925-6. PMID: 34969401

Yusuf NM, Zulkefli J, Jiram AI, Vythilingam I, Hisam S, Devi R, Salehuddin A, Ali NM, Isa M, Alias N, Ogu Salim N, Aziz AA, Sulaiman LH. *Plasmodium spp.* in macaques, *Macaca fascicularis*, in Malaysia, and their potential role in zoonotic malaria transmission. *Parasite.* 2022;29:32. doi: 10.1051/parasite/2022032. Epub 2022 Jun 8. PMID: 35674419

Case 2

Johanna Rigas^a DVM, MS, DACVP (clinical), Christine Watson^a DVM, MS, DACVP (anatomic), Anil Pattaswamy^a BVSc, MVSc, DVSC, DABT, Lisa Mullaney^b DVM, Elise LaDouceur^b DVM, DACVP (anatomic), Lisa Haviland^a DVM, Laure Molitor^a DVM

^aAltasciences Preclinical, Everett, WA, USA

^bThe Joint Pathology Center, Silver Spring, MD, USA

Clinical History: An approximately 2.5-year-old intact female colony Mauritius cynomolgus macaque was presented for veterinary assessment of an approximately 4 cm diameter subcutaneous, spherical, firm, slightly mobile ulcerated, rapidly enlarging mass in the left abdominal region. The animal was treated with a subcutaneous dose of Excede and administered topical Vetericyn. After one week with no improvement, cytologic aspirates were evaluated and samples were submitted for bacterial and fungal cultures.

Cytologic Description: Samples were moderately cellular with considerable hemocontamination. There was a population of spindle cells demonstrating mild to moderate anisocytosis and anisokaryosis with cells extending into long cytoplasmic tendrils. Nuclei were oval, composed of fine granular chromatin with one or multiple small nucleoli, and rare binucleation or micronuclei were seen. Cells were occasionally associated with amorphous magenta material (matrix). Moderate numbers of mixed inflammatory cells were present with predominance of mostly non-degenerate neutrophils. Rare intracellular and extracellular cocci microorganisms were identified. Occasional erythrophagia was observed, and rare hematoidin crystals were seen. The findings were consistent with a mesenchymal cell proliferation and septic mixed (primarily suppurative) inflammation with evidence of hemorrhage. Microscopic images of cytology samples are provided in figure 1.

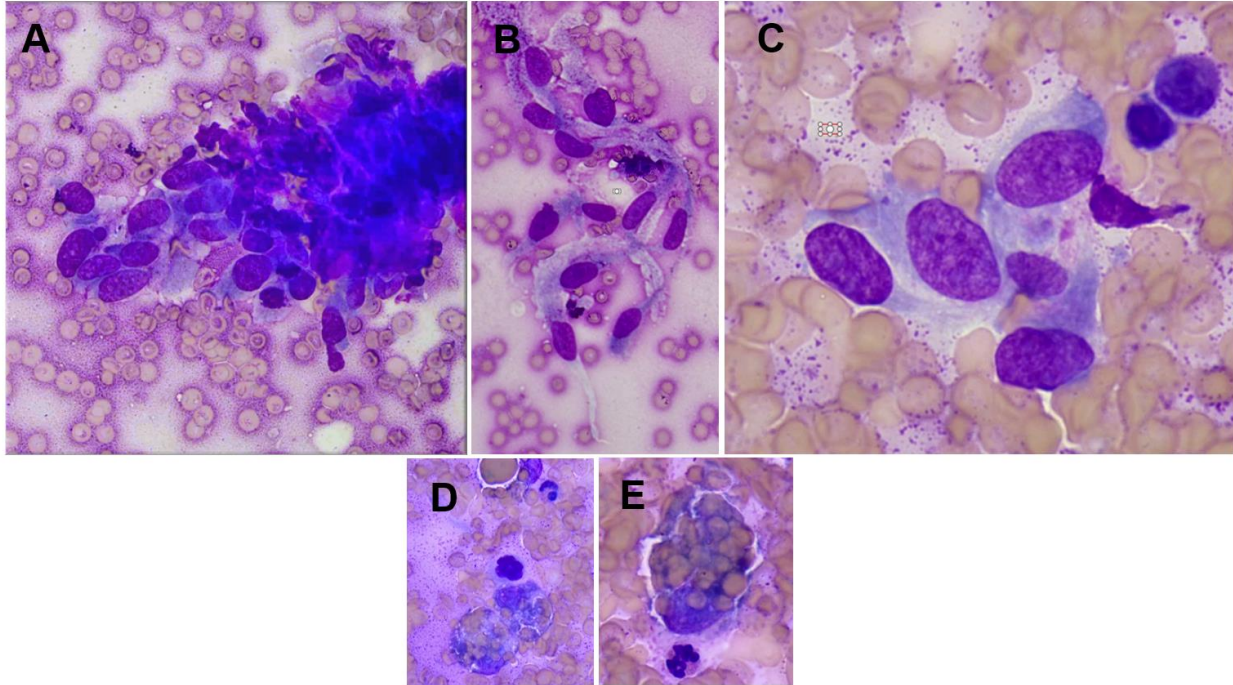


Figure 1. Microphotographs of cytology samples. (A) spindle cell aggregate with matrix material. Wright Giemsa, 50X objective. (B) individualized elongate spindle cells. Wright Giemsa, 50X objective. (C) one or multiple small nucleoli. Wright Giemsa, 100X objective. (D and E) erythrophagia, Wright Giemsa, 100X objective.

No bacterial organisms were isolated in aerobic culture. Histology was recommended, and the lesion was surgically excised.

Histologic Description: Expanding and effacing the dermis and subcutis, and elevating and extending to the epidermis there was a large, round, partially encapsulated, well demarcated and highly cellular neoplasm arranged in long streams and bundles of neoplastic spindle cells on a fine fibrovascular stroma. Neoplastic cells had indistinct cell borders, mild amount of cytoplasm, a round to oval or fusiform nucleus, and 1 to 2 distinct nucleoli with finely stippled chromatin. Mitotic figures were up to 18 per 2.37 mm^2 , with minimal anisocytosis and minimal to mild anisokaryosis. Throughout the neoplasm there were multifocal Antoni A and Antoni B neoplastic cells with variable Verocay bodies. There were multifocal and small numbers of lymphocytes and plasma cells, small numbers fragmented skeletal muscle fibers with rare regenerative skeletal muscle fibers, multifocal and small numbers of small caliber blood vessels (neovascularization), multifocal and minimal hemorrhage, multifocal and minimal edema (clear spaces), and multifocal areas of fibrillary eosinophilic material (collagen) that often separated neoplastic cells. The epidermis contained mild hyperplasia and had numerous blunted rete peg formations. The remaining epidermis was ulcerated admixed with multifocal to coalescing islands of basophilic cocci. Neoplastic cells extended to the end of the section. The lesion was consistent with a soft tissue sarcoma, and immunohistochemical assessment was performed for further characterization. Microscopic images of histology are provided in figure 2.

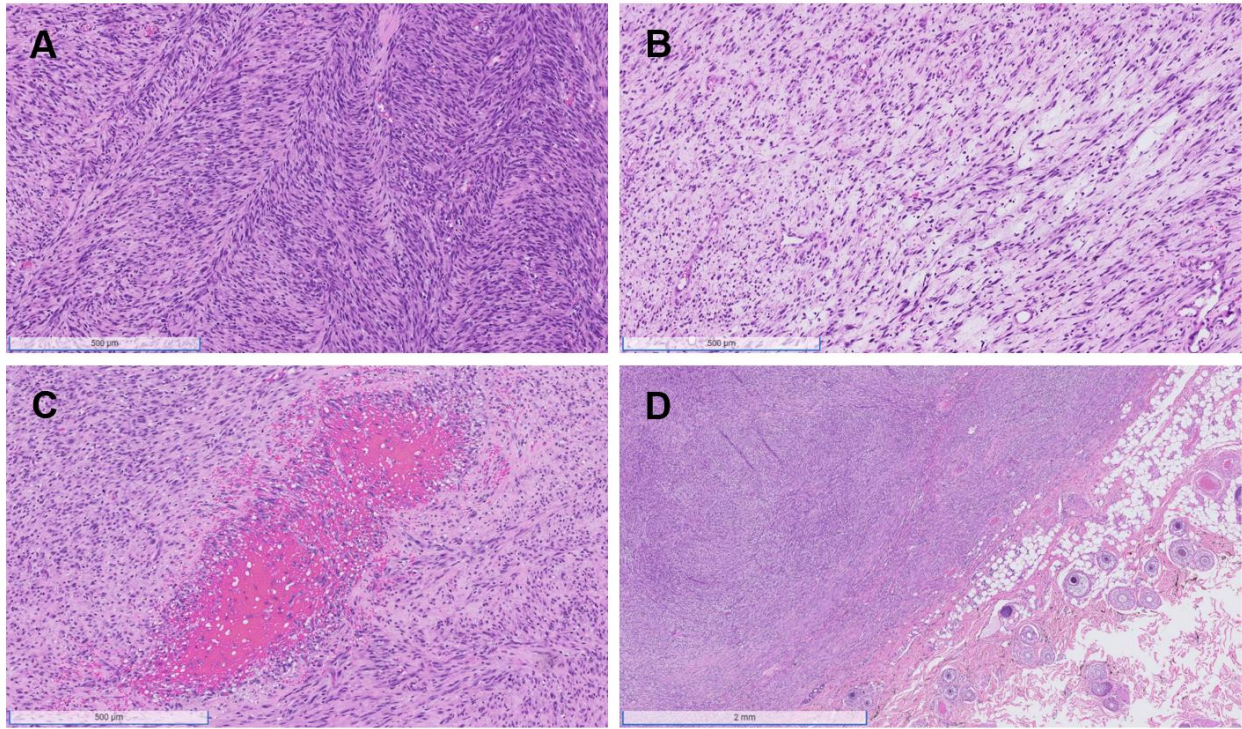


Figure 2. Images of histologic sections of subcutaneous mass. (A) Demonstrating Antoni A arrangement. HE, Bar= 500 µm. (B) Demonstrating Antoni B arrangement. HE, Bar= 500 µm. (C) Demonstrating hemorrhage and necrosis. Bar= 500 µm. (D) Demonstrating cutaneous interface. Bar= 2 mm.

Immunohistochemistry: Immunohistochemical reactivity to select markers are highlighted in Table 1. In summary, the neoplastic cell population exhibited strong diffuse immunoreactivity to vimentin, S100, CD56, collagen IV with approximately 40% of cells exhibiting immunoreactivity to SOX10. The neoplastic cells were diffusely immunonegative for melan-A, pan-actin, desmin, tyrosinase, microphthalmia associated transcription factor (MITF), and human melanoma black (HMB45). There were inconclusive results for CD34, and smooth muscle actin due to inappropriate negative and/or positive controls. Based on cellular morphology and immunohistology, the neoplasm was characterized as a nerve sheath tumor. Microscopic images of histologic sections for IHC are provided in figure 3.

Positive	Negative	Inconclusive
CD56	Desmin	Smooth muscle actin
SOX10	Pan-actin	CD34
Vimentin	Melan A	Fontana Masson
S100	Tyrosinase	
Collagen IV	MITF	
	HMB45	

Table 1. Immunohistochemistry reactivity summary.

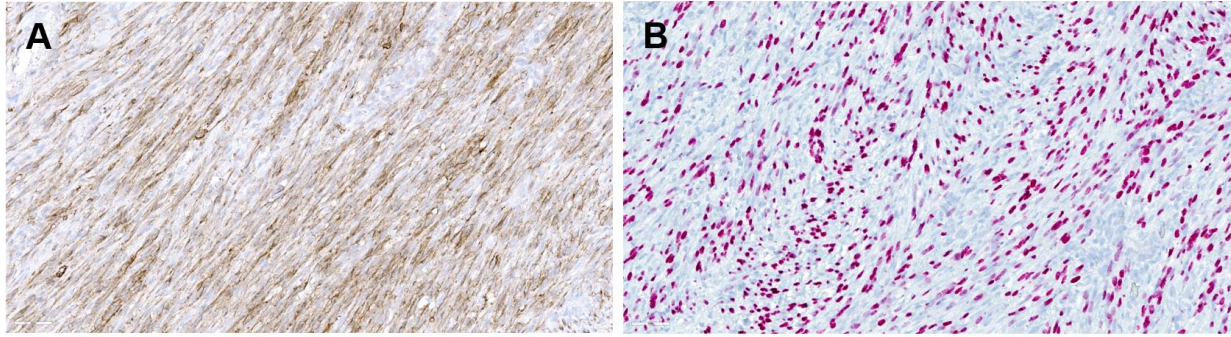


Figure 3. Images of histologic sections of subcutaneous mass (a) CD56 positive immunoreactivity. HE, Bar= 60 µm. (b) SOX10 positive immunoreactivity. HE, Bar= 60 µm.

Discussion: Cynomolgus macaque (CM) non-human-primates (NHP) are commonly utilized in pharmaceutical discovery and safety and efficacy toxicology studies.¹ Even though this species is commonly utilized for scientific studies, there are only small numbers of reports highlighting spontaneous neoplasms research NHP species.^{2,3} It is reported that majority of spontaneous neoplasms in the CM are of epithelial origin, specifically of endocrine, respiratory, and female reproductive systems. Although not directly related, in a report highlighting spontaneous neoplasms in the two populations of captive rhesus macaque NHPs (also commonly utilized in pharmacological studies), neoplasms of gastrointestinal origin were the most common with <1% incidence of neural origin neoplasia; there is one case report of a schwannoma characterized from an adult rhesus macaque.^{3,4}

Nerve sheath tumors (NST) are a category of soft tissue sarcoma (STS) which arise from components of cells associated with peripheral nerves including Schwann cells, fibroblasts, and other perineural cells. These have been reported in numerous domestic species and are most well characterized in dogs.^{5,6,7} A general classification of neoplasms arising from peripheral nerve sheath components in both veterinary species and humans consists of benign NSTs, schwannoma, neurofibroma, perineuroma, and malignant nerve sheath tumors (MNST).⁵⁻¹¹ Variations of benign NSTs and MNSTs are subcategorized in humans by histologic features, immunohistochemical (IHC) reactivity, ultrastructural analysis, and genetic markers indicating somatic or germline mutations. Few subclassification schemes are reported for veterinary species, yet benign NST/MNSTs may be further subdivided based on histologic features including grade, cell types, and IHC reactivity.

Histologic examination of hematoxylin and eosin-stained slides is often insufficient for the differentiation of STSs due to overlapping features, and PNSTs can be challenging to differentiate from one another as well as from other STSs such as perivascular wall tumors (PWT).

Immunohistochemistry has been employed for further characterization of these neoplasms in dogs with markers including, but not limited to, Sry-related HMg-Box gene 10 (SOX10), laminin, collagen IV, periaxin-1, claudin-1, glial fibrillary acidic protein (GFAP), and Ki-67, and in humans with numerous markers including S-100, SOX10, CD34, CD56, and calretinin.⁶⁻¹² It has been illustrated that laminin, SOX10, and periaxin-1 may help to differentiate canine PNST from PWT, and approximately 90%, 92% and 100% of canine benign PNSTs are immunoreactive for SOX10, claudin-1, and GFAP, respectively.^{6,7}

For the CM STS demonstrated in this case report, histologic features and immunoreactivity of IHC markers were evaluated with considerations for marker selection based on both veterinary and human literature. Positive vimentin immunoreactivity supported a neoplasm of mesenchymal origin, and S100, SOX10, collagen IV, and CD56 positive immunoreactivity provided evidence for a neoplasm of nerve sheath origin. In veterinary pathology, NSTs are subclassified as “malignant NST” when they are arising from a large nerve (e.g. brachial plexus), have “extremely large nuclei,” and/or contain areas of necrosis and hemorrhage (present in the current case). In contrast, in human pathology, NSTs are subclassified as “malignant NST” based on hypercellularity and generally >4 mitotic figures per 10HPF, both of which are present in the submitted tumor (the mitotic count was 18 per 2.37mm²).^{5,13} As there are different criteria for MNST subclassification between veterinary species and humans, and there is limited information for classification of NST/MNSTs in CM NHPs, the more general “nerve sheath tumor” diagnosis was favored. A spindle cell melanoma and a neoplasm of muscle origin were considered as differential diagnoses, and negative immunoreactivity for Melan A, tyrosinase, MITF, and HMB45 assisted to rule out a neoplasm of melanocytic origin, and a neoplasm of muscle cell origin was considered unlikely based on negative immunoreactivity for desmin and actin. This report may be the first to characterize a nerve sheath origin neoplasm in a CM.

References

1. Cynomolgus Macaques (*Macaca Fascicularis*) in Biomedical Research. *Nonhuman Primate Species at the National Primate Research Centers*, nprcresearch.org/primate/species.php. Accessed 20 Sept. 2023.
2. Kaspereit J, Friderichs-Gromoll S, Buse E, Habermann G. Spontaneous neoplasms observed in cynomolgus monkeys (*Macaca fascicularis*) during a 15-year period. *Exp Toxicol Pathol*. 2007;59(3-4):163-9.
3. Simmons HA, Mattison JA. The incidence of spontaneous neoplasia in two populations of captive rhesus macaques (*Macaca mulatta*). *Antioxid Redox Signal*. 2011;14(2):221-7.
4. Alves DA, Bell TM, Benton C, Rushing EJ, Stevens EL. Giant thoracic schwannoma in a rhesus macaque (*Macaca mulatta*). *J Am Assoc Lab Anim Sci*. 2010;49(6):868-72.
5. Higgins RJ, Bollen AW, Dickenson PJ, Siso-Llonch S. In: Tumors of the Nervous System. *Tumors in Domestic Animals*, 5th ed., Meuten D, ed. Wiley-Blackwell; 2017:834-891.
6. Sisó S, Marco-Salazar P, Roccabianca P, Avallone G, Higgins RJ, Affolter VK. Nerve Fiber Immunohistochemical Panel Discriminates between Nerve Sheath and Perivascular Wall Tumors. *Vet Sci*. 2022;10(1):1.
7. Tekavec K, Švara T, Knific T, Gombač M, Cantile C. Histopathological and Immunohistochemical Evaluation of Canine Nerve Sheath Tumors and Proposal for an Updated Classification. *Vet Sci*. 2022;9(5):204.
8. Chikkannaiah P, Boovalli MM, Nathiyal V, Venkataramappa S. Morphological spectrum of peripheral nerve sheath tumors: An insight into World Health Organization 2013 classification. *J Neurosci Rural Pract*. 2016;7(3):346-54.

9. Rodriguez FJ, Folpe AL, Giannini C, Perry A. Pathology of peripheral nerve sheath tumors: diagnostic overview and update on selected diagnostic problems. *Acta Neuropathol.* 2012;123(3):295-319.
10. Jaiswal P, Cd A, John JJ. A Spectrum of Histomorphological and Immunohistochemical Expression Profiles of S-100, CD56 and Calretinin in Benign Peripheral Nerve Sheath Tumours. *Cureus.* 2023;15(6):e40751.
11. Guedes-Corrêa, José, Cardoso, Rodrigo. Immunohistochemical Markers for Schwannomas, Neurofibromas and Malignant Peripheral Nerve Sheath Tumors-What Can the Recent Literature Tell Us?. *Arquivos Brasileiros De Neurocirurgia*, 2018;37:105-112.
12. Ramos-Vara JA, Borst LB. In: Immunohistochemistry: Fundamentals and applications in oncology. *Tumors in Domestic Animals*, 5th ed., Meuten D, ed. Wiley-Blackwell; 2017:44-87.
13. AFIP Atlas of Tumor Pathology, Fourth Series, Fascicle 19. *Tumors of the Peripheral Nervous System*. C. R. Antonescu, B. W. Scheithauer, & J. M. Woodruff. Washington, DC: Armed Forces Institute of Pathology, 2013: 396.

Elliott Chiu, DVM, MS, PhD
Anatomic pathology resident III
University of California, Davis; San Diego Zoo Wildlife Alliance
eschiu@ucdavis.edu; echiu@sdzwa.org

Slide: 23B1370 T1

Signalment: a 47 kg, adult, female chimpanzee (*Pan troglodytes*)

History: This female chimpanzee presented for a routine health check, whereupon a large, right renal mass was incidentally documented on ultrasound and palpation. The mass was surgically removed by performing a total nephrectomy.

Gross description: The kidney measured 14.8 x 11.8 x 11.4 cm and weighed 1.22 kg (Figure 1). The renal architecture was largely effaced with a single pole visible (Figure 1). The mass was completely encapsulated and contained by the renal capsule. On section, the mass nearly extended to periphery of kidney, effacing and replacing up to 80% of the normal renal parenchyma. Two gross morphologies were noted separated by a band of fibrous tissue interpreted as a scar, 1) a bulging, tan, relatively homogeneous nodule comprised 1/3 of the mass, was eccentrically located between the remainder of the mass and the normal renal parenchyma and 2) flat and tan tissue with red tracts of blood and vessels radiating from the central scar, representing 2/3 of the neoplasm.

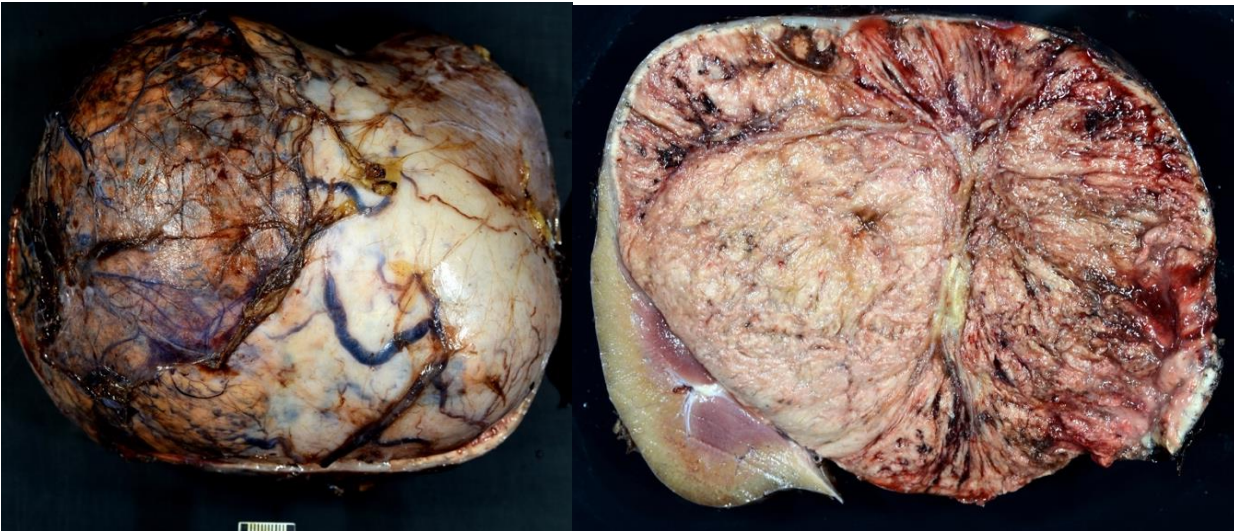


Figure 1: Gross photographs

Microscopic findings: Histology revealed an encapsulated, nodular, expansile, densely cellular, homogeneous mass comprised of neoplastic cells organized in moderately sized lobules, delineated by a delicate fibrovascular network. Neoplastic cells were polygonal with distinct cell borders, abundant, eosinophilic granular cytoplasm forming a chicken wire appearance. Nuclei were round with a peripheralized chromatin pattern, and generally indistinct nucleoli. Rare tubules were present lined by columnar epithelium with a brush border. There are occasional multinucleate cells with up to 4 nuclei. Anisocytosis was mild and anisokaryosis was mild to moderate. The mass was regionally interrupted by vessels and linear tracts of extravasated red blood cells that were grossly appreciated. Hemosiderophages were scattered throughout the mass. The mass extends to the renal capsule, which measures 7.5 microns.

Diagnosis: Kidney: oncocytoma

Discussion: Renal tumors in chimpanzees are rare. In a 2009 survey of two chimpanzee facilities including all reports of chimpanzee neoplasia prior to 2009, only four renal tumors were identified (n=117; 3.4%), including a primary renal carcinoma (Greenwood et al., 1995), an ectopic adrenal cortical carcinoma (Lowenstine, 1996), and two benign hemangiomas (Brown et al., 2009). Oncocytomas, or their malignant counterpart renal chromophobe cell carcinoma, have not been documented to date.

The immunohistochemical profile assisted diagnosis of an oncocytoma, while ruling out a renal chromophobe cell carcinoma. Neoplastic cells showed moderate to strong, cytoplasmic and membranous immunoreactivity to cKIT (CD117) throughout the mass (Figure 2A). Fewer than 1% of the neoplastic cells had moderate cytoplasmic immunoreactivity to CK7 (Figure 2B). In people, malignant transformation of an oncocytoma to a renal chromophobe cell carcinoma is generally coupled with the acquisition of marked CK7 expression (Wobker and Williamson, 2017; Zhao et al., 2015). While complete negative CK7 staining is regarded to be less supportive of an oncocytoma, rare (fewer than 5%), random neoplastic cell-immunoreactivity to CK7 is considered typical for oncocytoma (Williamson et al., 2017).

Other markers, including DOG1, cyclin D1, vimentin, and special stains, including colloidal iron, SDH have been used in human medicine (Williamson et al., 2017; Zhao et al., 2015), but were not deemed necessary in this case. DOG1 is uniformly expressed in chromophobe renal cell carcinoma and oncocytomas, but absent in clear cell renal cell carcinomas. Cyclin D1 is variably expressed in oncocytomas, but not expressed in either carcinoma. Vimentin is variably expressed in oncocytomas and clear cell renal cell carcinoma, but negative in chromophobe renal cell carcinomas (Zhao et al., 2015). SDH is used as a marker of differentiation between oncocytomas and renal chromophobe cell carcinomas in cases where morphology is not clear; though it is not used as a screening marker (Williamson et al., 2017).

An oncocyte does not refer to a particular cell of origin or histogenesis, but rather, it serves as a morphologic cellular description for a histologic change that can occur to cells in any organ (Tallini, 1998). Namely, an oncocyctic change/transformation is characterized by cytomegaly coupled with an abundant eosinophilic granular cytoplasm due to the accumulation of altered mitochondria making up 30 to 60% of the cytoplasmic volume, presumably the result of metabolic or cellular stress (Asa, 2004; Tallini, 1998). Some cells may normally have increased numbers of mitochondria, and so evaluation must include the cell of origin.

Transmission electron microscopy identified eosinophilic granules within the cytoplasm as mitochondria. In a 70 nm tissue section, the cytoplasm of neoplastic cells contained 50 to 100, round to oval, irregular, 500 nm to 1-micron-diameter, occasionally fractured, double membrane-bound mitochondria with tubular, haphazardly arranged cristae surrounded by variable amounts of clear space (Figure 2C and 2D). No other organelles were readably identified. The nuclei were often round to indented with few crenated and convoluted nuclei with mixed euchromatin and heterochromatin and lacked a nucleolus. The cell membrane was generally smooth with small pockets of microvilli at the intersection between neighboring cells. In the case of renal oncocytomas, the cell of origin is believed to be the intercalated cell of the cortical portion of the distal collecting duct (Skinnider and Amin, 2005).

Oncocytomas in humans represent 3 to 7% of all primary renal tumors (Rosenkrantz et al., 2010). Beyond their characteristic gross, histologic, immunohistochemical, and ultrastructural features, human oncocytomas have been further evaluated karyotypically or by fluorescent in situ hybridization. Changes include a diploid karyotype, loss of chromosome 1, loss of Y, or rearrangement of 11q13 (Hes et al., 2016; Wobker and Williamson, 2017).

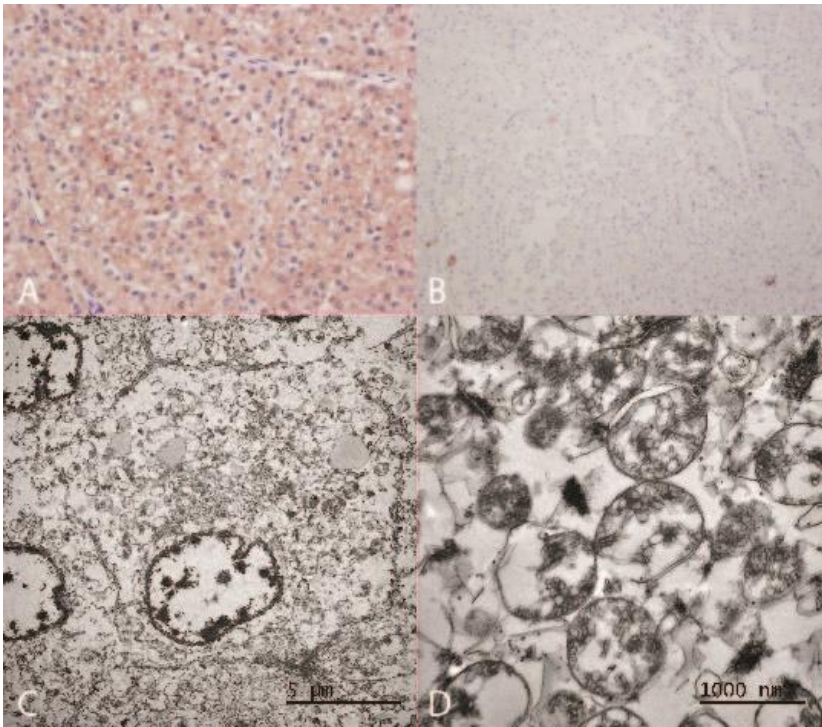


Figure 2: IHC and TEM of renal oncocytoma. A) c-Kit displays strong membranous and cytoplasmic immunoreactivity; B) CK7 shows cytoplasmic immunoreactivity in few cells; C and D) Neoplastic cells harbor dozens to hundreds of round-to-oval, fairly denatured mitochondria, with few other recognizable organelles.

References:

- Asa, S.L., 2004. My approach to oncocytic tumours of the thyroid, *J Clin Pathol*.
- Brown, S.L., Anderson, D.C., Dick, E.J., Guardado-Mendoza, R., Garcia, A., Hubbard, G.B., 2009. Neoplasia in the Chimpanzee (*Pan spp.*). *J Med Primatol* 38, 137–144.
- Eble, J.N., Hull, M.T., 1984. Morphologic features of renal oncocytoma: a light and electron microscopic study. *Hum Pathol* 15, 1054–1061.
- Greenwood, A.G., Lowe, J.W., Gaunt, L., 1995. Renal carcinoma in a chimpanzee (*Pan troglodytes*). *Veterinary Record* 137, 380–381.
- Hes, O., Moch, H., Reuter, V., 2016. Oncocytoma, in: Moch, H., Humphrey, P., Ulbright, T., Reuter, V.E. (Eds.), *WHO Classification of Tumours of the Urinary System and Male Genital Organs*. International Agency for Research on Cancer, Lyon, pp. 43–44.
- Lowenstine, L., 1996. Neoplasms and proliferative disorders in nonhuman primates, in: Benirschke (Ed.), *Primates: The Road to Self-Sustaining Populations*. Springer-Verlag, New York, pp. 781–814.
- Rosenkrantz, A.B., Hindman, N., Fitzgerald, E.F., Niver, B.E., Melamed, J., Babb, J.S., 2010. MRI features of renal oncocytoma and chromophobe renal cell carcinoma. *American Journal of Roentgenology* 195. <https://doi.org/10.2214/AJR.10.4718>
- Skinnider, B.F., Amin, M.B., 2005. An immunohistochemical approach to the differential diagnosis of renal tumors. *Semin Diagn Pathol* 22, 51–68. <https://doi.org/10.1053/j.semdp.2005.11.004>
- Tallini, G., 1998. Oncocytic tumors. *Virchows Archive* 433, 5–12.
- Williams, G.M., Lynch, D.T., 2023. Renal oncocytoma, in: StatPearls [Internet]. StatPearls Publishing, Treasure Island.
- Williamson, S.R., Gadde, R., Trpkov, K., Hirsch, M.S., Srigley, J.R., Reuter, V.E., Cheng, L., Kunju, L.P., Barod, R., Rogers, C.G., Delahunt, B., Hes, O., Eble, J.N., Zhou, M., McKenney, J.K., Martignoni, G., Fleming, S., Grignon, D.J., Moch, H., Gupta, N.S., 2017. Diagnostic criteria for oncocytic renal neoplasms: a survey of urologic pathologists. *Hum Pathol* 63, 149–156. <https://doi.org/10.1016/j.humpath.2017.03.004>
- Wobker, S.E., Williamson, S.R., 2017. Modern Pathologic Diagnosis of Renal Oncocytoma. *J Kidney Cancer VHL* 4, 1–12. <https://doi.org/10.15586/jkcvhl.2017.96>
- Zhao, W., Tian, B., Wu, C., Peng, Y., Wang, H., Gu, W.L., Gao, F.H., 2015. DOG1, cyclin D1, CK7, CD117 and vimentin are useful immunohistochemical markers in distinguishing chromophobe renal cell carcinoma from clear cell renal cell carcinoma and renal oncocytoma. *Pathol Res Pract* 211, 303–307. <https://doi.org/10.1016/j.prp.2014.12.014>



Oklahoma Animal Disease Diagnostic Laboratory

The Case of the Capuchin Monkey

Giselle Cino^{1*}, Laura Centurion¹, Scott Mitchell¹

1. Oklahoma Animal Disease Diagnostic Laboratory, Oklahoma State University, Stillwater, Ok 74074

Signalment:

2-year-old, female, capuchin monkey (*Cebus capucinus*).

History:

Found dead in enclosure with 7 other monkeys. No past health issues. Good body weight (2.3 kg) on last exam three months prior. Tuberculosis negative. Was received at current facilities 6 months prior from a zoo in Kansas. Suspect: accident/fall from perch to cement floor.

Gross Findings:

The cadaver is in poor body condition as evidenced by markedly reduced subcutaneous and visceral adipose tissue stores, reduced skeletal muscle mass, and prominent spinal, rib, and pelvic bone protuberances. Remaining adipose tissue adjacent to the kidneys and within the omentum is gelatinous and semi-translucent (serous atrophy of fat). There is approximately 30 mL of a yellow-tinged, clear, thin fluid within the thoracic cavity. Diffusely covering the pleura and pericardium and adhering the visceral pleura to the parietal pleura and the epicardium to the pericardium, respectively, is a thick membrane of pale tan, fragile, fibrillar material (fibrin), intermixed with occasional firm, difficult to break fibrous tags. In formalin-fixed sections of lungs, several approximately 0.1x1.5 cm, round, white adult nematodes are observed associated with the cut surface and within pleural fibrin mats. The lungs are diffusely mottled dark red and are collapsed. Within the left ventricular free wall, all liver lobes, renal parenchyma, and left occipital cerebral lobe are multifocal, 1-8 mm diameter, tan foci with a yellow/green mucopurulent center (abscesses). The left axillary lymph node is multifocally pigmented dark blackish.

Microscopic Findings:

The pleura and epicardium are diffusely and markedly expanded by moderate to large numbers of neutrophils, macrophages, lymphocytes, plasma cells, fewer multinucleated giant cells (pleura), and rare eosinophils, admixed with large amounts of organized fibrin, large amounts of fibrous tissue often forming thick bands, and multifocal colonies of Gram positive cocci, and several, up to 300 μm diameter, on their widest cross sections longitudinal and transverse cross sections of adult parasites, characterized by a 1 μm thick cuticle, coelomyarian-polymyarian musculature, and a celom containing reproductive structures (adult filariids). Visceral mesothelial cells are frequently swollen with vesiculate nuclei (hypertrophy).

Multifocally, randomly effacing the parenchyma of liver, kidney, left ventricular wall, and occipital brain lobe are variably sized, up to 5 mm diameter encapsulated lesions comprised of very large numbers of degenerate and non-degenerate neutrophils, admixed with large amounts of fibrin, cellular and karyorrhectic debris, moderate hemorrhage, and Gram positive cocci (abscesses).



Oklahoma Animal Disease Diagnostic Laboratory

Extensively effacing the mucosa of the nasal cavity, expanding the submucosa, infiltrating into the nasal conchae cartilage, and partially occluding the nasal cavity, are large numbers of degenerate neutrophils admixed with large amounts of fibrin, necrotic cellular debris, and Gram positive coccobacilli. Mucosa in the affected areas is extensively eroded or ulcerated. Affected cartilage is necrotic, characterized by locally extensive areas of hypereosinophilic, fragmented, and lost cartilaginous stroma and loss of chondrocytes within the lacunae. Small caliber blood vessels are frequently partially or completely occluded by fibrin thrombi.

Parasites: There are several, up to 300 μm diameter, longitudinal and transverse parasite cross sections characterized by a 1 μm thick cuticle and coelomyarian musculature, surrounding parenchyma containing reproductive structures (adult filariids).

Tonsil, lymph node, and spleen: Diffusely, there are markedly decreased numbers of lymphocytes and depleted lymphoid follicles with no germinal centers.

Diagnoses:

Pleura, pericardium: Fibrinosuppurative and proliferative polyserositis, diffuse, severe, chronic-ongoing, with intralesional Gram positive cocci.

Heart, kidney, liver, brain, nasal cavity: Disseminated necrosuppurative histiocytic, fibrosing myocarditis, nephritis, hepatitis, meningoencephalitis, and rhinitis,

Tonsil, lymph nodes, spleen: Lymphoid depletion, diffuse, severe.

Discussion:

Gross and histologic findings of disseminated abscesses, chronic lymphoplasmacytic inflammation within multiple organs, and polyserositis (pleuritis and pericarditis) are altogether consistent with septicemia, supported by the presence of intralesional Gram positive coccobacilli in all these tissues. The primary site of infection is presumed to be the respiratory tract. Aerobic cultures of the liver and pericardium isolated moderate numbers of *Staphylococcus aureus*, which is the suspected cause of septicemia in this case. *S. aureus* septicemia is supported by widespread lymphoid depletion; however, it is uncertain if the lymphoid depletion is secondary to septicemia or a primary immunodeficient disorder. Viral causes of immunodeficiency were not screened in this case. Primary *Staph aureus* infections are rarely reported in non-human primates, but it has been reported in immune-suppressed macaques. (1) Parasitology testing revealed the presence of spirurid parasites and eggs (Filarids), and Strongyles and Trichostrongyles eggs in fecal float. Respiratory filariid infection are common incidental findings in new world monkeys. (1,2) Route of infection requires inoculation of larvae from mosquitoes, which is the major reason they are uncommon in non-human primate colonies housed in closely controlled laboratory environments. Most common respiratory tract filariids identified in NWM are *Filaroides* sp. And *Filariopsis* sp. (1)



Oklahoma Animal Disease Diagnostic Laboratory

References:

1. Lowenstine LJ, Osborn KG. Respiratory System Diseases of Nonhuman Primates. *Nonhuman Primates in Biomedical Research*. 2012:413–81. doi: 10.1016/B978-0-12-381366-4.00009-2. Epub 2012 Mar 26. PMID: PMC7158299.
2. Narama, I. et. al., (1985). Microfilarial Granulomas in the Spleens of Wild-Caught Cynomolgus Monkeys (*Macaca fasciula c dx zris*). *VetPath*, 22:4 (355-362).

MICHIGAN STATE
U N I V E R S I T Y

Case 5: Black and White Ruffed Lemur SP12-0007896

CONTRIBUTOR(S)/ INSTITUTION:

Hunter Wojtas¹ and Dalen Agnew, DVM, PhD, Dipl ACVP¹

¹Michigan State University College of Veterinary Medicine, East Lansing, MI, 48824, USA

SIGNALMENT:

Twenty-six-year-old male black and white ruffed lemur (*Varecia variegata variegata*)

HISTORY:

This geriatric black and white ruffed lemur had been monitored for his body weight the last year and given nutritional supplements. He was on a biannual exam schedule and was last evaluated two years prior to death with no specific concerns. He has some documented spondylosis and cheek tooth wear. He was found dead on the cage floor by keeper staff. He was acting and eating normally the previous day.

GROSS FINDINGS:

Abdominal cavity: Hemoabdomen
Liver: Neoplasia; presumptive hemangiosarcoma



COLLEGE OF
**VETERINARY
MEDICINE**

**Department of
Pathobiology and
Diagnostic Investigation**

Michigan State University
4125 Beaumont Road
Room 201B
Lansing, MI
48910-8107
517-432-4685
FAX: 517-432-5836

MICHIGAN STATE UNIVERSITY

HISTOPATHOLOGIC AND CLINICAL PATHOLOGY FINDINGS:

The sections of liver contained a multilobulated proliferation of neoplastic hepatocytes arranged in sheets and thick cords (more than 5 hepatocytes thick) supported by fine fibrovascular stroma and lacking discernible bile ducts or portal architecture. Neoplastic cells had abundant cytoplasm and contained oval large nuclei with prominent nucleoli. Mitoses were 3 per 10 HPF, and there was marked anisocytosis and anisokaryosis. Multinucleated cells were frequently observed. There were multifocal areas of necrosis and hemorrhage. One of the liver sections contained non-neoplastic liver tissue which was characterized by multiple small regenerative nodules divided by interlobular bridging fibrosis, bile duct proliferation, and severe brown pigment deposition within the hepatocytes, biliary epithelium, and macrophages. There was locally extensive lymphocytic infiltration mainly located in portal tracts and bridging fibrosis. Occasionally, inspissated bile pigment were observed in the bile ducts.

Additionally, sections of heart, lung, spleen, stomach, intestinal tract, kidney, urinary bladder, trachea, and lymph node were evaluated. The gall bladder mucosa was severely thickened with cystic mucinous hyperplasia of overlying epithelium. Sections of lung had severe pulmonary edema characterized by accumulation of pale eosinophilic fluid material within the alveolar space and increased numbers of intraalveolar macrophages. Additionally, there was moderate lymphocytic infiltration with multiple lymphoid follicles, around the bronchioles and small arteries (BALT hyperplasia). The sections of kidney were characterized by diffuse accumulation of brown pigment in the renal tubular epithelium. There were multiple renal tubules containing eosinophilic fluid in the lumen. The glomeruli had various degree of thickening of basement membrane, and atrophic and sclerotic glomeruli were often noted. Occasionally, multifocal areas of linear interstitial fibrosis extending from the medulla to cortex were noted. The sections of intestinal tract were severely autolyzed; however, there was mixed inflammatory cell infiltration in the lamina propria.



COLLEGE OF
**VETERINARY
MEDICINE**

**Department of
Pathobiology and
Diagnostic Investigation**

Michigan State University
4125 Beaumont Road
Room 201B
Lansing, MI
48910-8107
517-432-4685
FAX: 517-432-5836

MORPHOLOGICAL/ETIOLOGICAL DIAGNOSIS:

Liver: Hemochromatosis; hepatocellular carcinoma

Additional diagnoses (tissues not provided):

Gall bladder: Mucinous and cystic hyperplasia

Lung: Pulmonary edema; mild perivascular lymphocytic infiltration

Kidney: Diffuse tubular hemosiderosis; multifocal mild interstitial fibrosis;
moderate membranoproliferative glomerulonephritis with proteinuria

DISCUSSION:

The histologic findings in the liver are consistent with hepatocellular carcinoma (HCC) and hemochromatosis. HCC has been reported in higher numbers in prosimians than other mammalian species, with the lungs as the most common site of metastasis.⁷ Grossly, these tumors may appear as variably sized masses and vary from individual to multiple invasive masses.⁴ Hepatocytes demonstrate marked pleomorphism and anisocytosis with low numbers of atypical mitotic figures.⁴ An exact cause for this higher incidence of HCC in lemurs has not been identified.

Some have suggested that hemochromatosis may cause hepatic neoplasia in lemurs, much like in human hereditary hemochromatosis, where HCC is a common sequela.^{2-3,6} Hemochromatosis is an overload of iron in the tissues that causes hepatic damage. This differs from hemosiderosis, where an abundance of iron deposition in tissues does not cause disease. Hemosiderosis has been reported more frequently in prosimians, although recent methods suggest this high incidence and pathogenic effect may be overstated.^{1,2} It has been proposed that dietary differences between captive and wild lemurs may be the reason for increased hemosiderosis of captive populations.⁶ Lemurs living in the wild eat more tannins, which chelate iron to prevent absorption, and lemurs in captivity eat more ascorbic acid, which converts iron from Fe³⁺ to the more bioavailable Fe²⁺.⁶ Because of these findings, adjustments to management of captive prosimians has been suggested by the AZA prosimian taxonomy advisory group.⁵ However, anecdotal accounts have found that changing the diet does not seem to decrease the number of captive lemurs with hepatic neoplasms.⁴ Additionally, recent studies in captive prosimians do not support the association between hemochromatosis and increased HCC, and they suggest the cause for increased HCC in lemurs is more complex.⁷ They also eliminated the possibility of hepadnavirus causing HCC and demonstrated lack of histologic changes to support aflatoxin B1 and chronic inflammation as associated with HCC.⁷ Interestingly, they found a novel trend between prosimians with spontaneous HCC and lower amounts of cobalamin levels.⁷ To understand the cause of this fatal disease in these important populations, further studies are necessary.



COLLEGE OF
**VETERINARY
MEDICINE**

**Department of
Pathobiology and
Diagnostic Investigation**

Michigan State University
4125 Beaumont Road
Room 201B
Lansing, MI
48910-8107
517-432-4685
FAX: 517-432-5836

REFERENCES:

1. Glenn KM, Campbell JL, Rotstein D, Williams CV. Retrospective evaluation of the incidence and severity of hemosiderosis in a large captive lemur population. *Am J Primatol.* 2006;68:369-381.
2. Gonzales J, Benirschke K, Saltman P, Roberts J, Robinson PT. Hemosiderosis in lemurs. *Zoo Biol.* 1984; 3:255-265.
3. Kane SF, Roberts C, Paulus R. Hereditary Hemochromatosis: Rapid Evidence Review. *Am Fam Physician.* 2021;104:263-270.
4. McAloose D, Stalis IH. Chapter 13 - Prosimians. In: Terio KA, McAloose D, Leger JS, eds. *Pathology of Wildlife and Zoo Animals.* 1st ed. Academic Press; 2018.
5. Prosimian Taxon Advisory Group. Iron Storage Disease in Lemurs. St. Louis Zoo, St. Louis, Missouri: PTAG meeting on iron storage disease; 2003.

Accessed September 29, 2023. <https://nagonline.net/wp-content/uploads/2013/12/PTAGIronReccsfinal1.pdf>

6. Spelman LH, Osborn KG, Anderson MP. Pathogenesis of hemosiderosis in lemurs: Role of dietary iron, tannin, and ascorbic acid. *Zoo Biol.* 1989;8:239-251.
7. Zadrozny LM, Williams CV, Remick AK, Cullen JM. Spontaneous Hepatocellular Carcinoma in Captive Prosimians. *Vet Pathol.* 2010;47:306-311.

MICHIGAN STATE
UNIVERSITY

Ring-Tailed Lemur SZ21-0014868

CONTRIBUTORS/ INSTITUTION:

Megan Crawford¹ and Dalen Agnew, DVM, PhD, Dipl ACVP¹

¹Michigan State University College of Veterinary Medicine, East Lansing, MI, 48824, USA

SIGNALMENT:

4-year-old, male intact ring-tailed lemur (*Lemur catta*)

HISTORY:

This captive-born ring-tailed lemur from a zoo had a six-day history of reduced appetite and lethargy. Bloodwork revealed elevated liver enzymes, hyperbilirubinemia, and toxic changes to white blood cells. Despite treatment with enrofloxacin, fluid therapy, prednisolone, and tramadol, this animal continued to decline and was found dead.

GROSS FINDINGS:

The necropsy was performed at the referring zoological institution. The liver appeared enlarged, pale pink, had petechiae on the surface, and was friable. The cecum and proximal colon contained a large amount of gas. Blood vessels of the duodenum were prominent. There was a moderate amount of ingesta in the stomach. There was 40 mL of a clear yellow pleural effusion. The lungs were wet, heavy, and had a mottled pink to red appearance. Pericardial fat was translucent and gelatinous. The trachea and mouth contained a foamy liquid. The kidneys were pale. There was a small amount of dark yellow flocculent urine in the bladder. No other gross findings were noted.



COLLEGE OF
**VETERINARY
MEDICINE**

**Department of
Pathobiology and
Diagnostic Investigation**

Michigan State University
4125 Beaumont Road
Room 201B
Lansing, MI
48910-8107
517-432-4685
FAX: 517-432-5836

HISTOPATHOLOGIC FINDINGS:

In the liver and spleen, there were multifocal random variably sized areas of necrosis with fibrin and neutrophils. Scattered protozoal schizonts and some large protozoal cysts with bradyzoites were in rare areas of necrosis. Several randomly scattered small irregular glial nodules were within the cerebral neuropil. The pulmonary alveolar septa were mildly thickened, and the lungs were congested.

MORPHOLOGICAL/ETIOLOGICAL DIAGNOSIS:

Liver: Severe multifocal necrotizing hepatitis with intralesional protozoa

Spleen: Severe multifocal necrotizing splenitis

Brain: Mild multifocal encephalitis

Lung: Mild interstitial pneumonia

Immunohistochemistry for *Toxoplasma gondii*: Positive

DISCUSSION:

Histologic and ancillary testing was consistent with disseminated toxoplasmosis. *Toxoplasma gondii* is an apicomplexan parasite, with ingested oocysts shed by cats being the source of infection.^{2,3} Felines serve as the definitive host for *T. gondii* and unsporulated oocysts are shed in affected felines' feces.⁴ Sporulated oocysts can contaminate food, especially meat. The oocysts may also be ingested by intermediate hosts through consumption of water or raw vegetables. Intermediate hosts include susceptible mammals, such as the ring-tailed lemur. *Toxoplasma gondii* has also been shown to be transmitted through the placenta to the fetus in the tachyzoite form.¹ The presence of this parasite induces an antibody response but may not cause clinical disease until the animal is in an immunosuppressed state, such as with stress, concurrent infection, or pregnancy. The presence of felids in a zoological institution can serve as a source of infection for highly susceptible species, such as the ring-tailed lemur. Although the source of infection for this case is unknown, it is recommended zoological institutions housing ring-tailed lemurs practice strict hygiene and avoid feeding fresh raw meat to felids because this may be a source of *T. gondii* ingestion. Additionally, as much distance as possible should be kept between felid and ring-tailed lemur exhibits.

REFERENCES:

1. Juan-Sallés C, Mainez M, Marco A, Sanchís AM. Localized toxoplasmosis in a ring-tailed lemur (*Lemur catta*) causing placentitis, stillbirths, and disseminated fetal infection. *J Vet Diagn Invest.* 2011 Sep;23(5):1041-5.
2. Rocchigiani G, Fonti N, Nardoni S, Cavicchio P, Mancianti F, Poli A. Toxoplasmosis in Captive Ring-Tailed Lemurs (*Lemur catta*). *Pathogens.* 2022 11:1142.
3. Spencer JA, Joiner KS, Hilton CD, Dubey JP, Toivio-Kinnucan M, Minc JK, Blagburn BL. Disseminated toxoplasmosis in a captive ring-tailed lemur (*Lemur catta*). *J Parasitol.* 2004; 90:904-6.
4. Centers for Disease Control and Prevention. CDC - Toxoplasmosis. Accessed 29 Aug. 2018. www.cdc.gov/parasites/toxoplasmosis/.



COLLEGE OF
**VETERINARY
MEDICINE**

**Department of
Pathobiology and
Diagnostic Investigation**

Michigan State University
4125 Beaumont Road
Room 201B
Lansing, MI
48910-8107
517-432-4685
FAX: 517-432-5836

MICHIGAN STATE
UNIVERSITY

Case 7

Lemur SP10-0006530

CONTRIBUTOR(S)/ INSTITUTION:

Abigail Smith,¹ Dalen Agnew, DVM, PhD, Dipl ACVP¹

¹*Michigan State University College of Veterinary Medicine, East Lansing, MI, 48824, USA*

SIGNALMENT:

12-year-old male Ring-tailed Lemur (*Lemur catta*)

HISTORY:

An adult male ring-tailed lemur presented with labored breathing. A large pulmonary mass was noted on radiographs. It did not recover well from anesthesia and was euthanized.



**COLLEGE OF
VETERINARY
MEDICINE**

Department of
**Pathobiology
& Diagnostic
Investigation**

Michigan State University
Veterinary Medical Center
784 Wilson Road
Rm. D208
East Lansing, MI
48824

PH:517-432-4685
www.pathobiology.msu.edu

GROSS FINDINGS:

A 9 cm diameter X 7 cm long gelatinous mass was present in the pleural cavity replacing most of the normal lung parenchyma. The liver had a raised 1 cm firm nodule on one lobe. Clear fluid was present in the abdominal cavity.

HISTOPATHOLOGIC AND CLINICAL PATHOLOGY FINDINGS:

The lung tissue is largely replaced by large thick-walled fibrous cavities with abundant lymphoplasmacytic nodular aggregates, macrophages, neutrophils, and eosinophils expanding the walls and adjacent pulmonary parenchyma. Within many cavities are large viable and degenerate larval cestodes characterized by their segmented integument, calcareous corpuscles, a scolex with a rostellum bearing hooklets, and spinous tegument. In the remaining lung, there were multifocal areas of parenchymal collapse of airways, peripheral emphysema, and pools of neutrophils, fibrin, and hemosiderin laden macrophages in alveolar spaces and within capillaries. Many megakaryocytes were also circulating in the capillaries.

Additional sections of liver, kidney, spleen, diaphragm, gallbladder, intestine, heart, lymph node, pancreas, and trachea. Small nodular areas of inflammation are noted on the serosa of the intestine and on the diaphragm. The liver has diffusely widely dilated sinusoids, a markedly undulating hepatic capsule, and large spaces filled with hemorrhage and fibrin. Tubules within the kidney, particularly in the deep medulla, have protein and cellular casts. Small granular pigment deposits are scattered in the tubular epithelial cytoplasm. In the heart, at the outflow point of a large valve (unidentified), there is a focal area of atherosclerosis characterized by disruption of the lamina by foamy swollen cells.

MORPHOLOGICAL/ETIOLOGICAL DIAGNOSIS:

Lung: Severe granulomatous and fibrous pleuropneumonia with intralesional larval cestodes (presumptive *Cysticercus longicollis*, the larval form of *Taenia crassiceps*)

DISCUSSION:

The findings in the lung are most suggestive of pulmonary cysticercosis. There are few cases of cysticercosis caused by *Cysticercus longicollis* that have been described in lemurs.^{1,2,3,5} Domestic and wild canids are the definitive host of the cestode *Taenia crassiceps*, in which eggs are passed in the feces and then ingested by the intermediate host, typically rodents.² It has also been found that the cysticerci can be transmitted by intraperitoneal passage and cannibalism in laboratory mice.^{2,4} In this case, the lemur was housed at a zoo with potential for direct contact with a rodent or indirect contact with a canid species through contaminated food or other fomites; however, it is unclear how this lemur was infected. *Cysticercus longicollis*, is highly invasive due to its ability to go through exogenous and endogenous budding.² In this case, and one other reported case of a ring-tailed lemur, lesions were isolated to the thoracic cavity.¹ Clinical signs seem to be variable: in our case the lemur had labored breathing; whereas, the other lemur had acutely died without any observed clinical signs.¹ Lesions found in different parts of the body are histologically similar including cyst-like or cavitated masses with granulomatous inflammation and numerous larvae inside.^{1,2,5} In one study, larvae were collected to sequence the DNA; perhaps this may be an option for earlier detection in lemurs.¹

REFERENCES:

1. Alić A, Hodžić A, Škapur V, Alić SS, Prašović S, Duscher GG. Fatal pulmonary cysticercosis caused by *Cysticercus longicollis* in a captive ring-tailed lemur (*Lemur catta*). *Vet Parasit*, 2017; 241:1-4.
2. Dyer, NW, Greve JH. Severe *Cysticercus longicollis* cysticercosis in a black lemur (*Eulemur macaco macaco*). *J Vet Diag Invest*, 1998; 10:362-364.
3. Hofmannova L, Mikes L, Jedlickova L, Pokorny J, Svobodova V. Unusual cases of *Taenia crassiceps* cysticercosis in naturally animals in the Czech Republic. *Veterinarni Medicina*. 2018;63: 73–80.
4. Sitali MC, Schmidt V, Mwenda R, Sikasunge CS, Mwape KE, Simuunza MC, da Costa CP, Winkler AS, Phiri IK. Experimental animal models and their use in understanding cysticercosis: A systematic review. *PLoS One*. 2022;17:e0271232.
5. Young LA, Morris PJ, Keener L, Gardiner CH, Stalis IH, Bicknese E, Sutherland-Smith M, Janssen DL. Subcutaneous *Taenia crassiceps* cysticercosis in a red ruffed lemur (*Varecia variegata rubra*). *IAAAM Archive*, 2000.

Acknowledgments:

We thank the veterinary and keeper staff at Cincinnati Zoo for their care of this lemur and providing case history.

MICHIGAN STATE
UNIVERSITY

Case 8

Lemur DA101976

CONTRIBUTOR(S)/ INSTITUTION:

Dalen Agnew, DVM, PhD, Dipl ACVP, ¹ Anneke Moresco, DVM, PhD²

¹Michigan State University College of Veterinary Medicine, East Lansing, MI, 48824, USA, ²Reproductive Health Surveillance Program

SIGNALMENT:

29-year-old female Ring-tailed Lemur (*Lemur catta*)

HISTORY:

This lemur's reproductive tract was submitted to the AZA Reproductive Health Surveillance Program archive. It was euthanized due to progressive weight loss, suspected fibrosarcoma on chest wall, flaccid tail, and a positive titer to coccidioidomycosis. There was no record of any pregnancies or contraception.



**COLLEGE OF
VETERINARY
MEDICINE**

Department of
**Pathobiology
& Diagnostic
Investigation**

Michigan State University
Veterinary Medical Center
784 Wilson Road
Rm. D208
East Lansing, MI
48824

PH:517-432-4685
www.pathobiology.msu.edu

GROSS FINDINGS:

Only the reproductive tract was available and was grossly within normal limits.

HISTOPATHOLOGIC AND CLINICAL PATHOLOGY FINDINGS:

Sections of cervix, uterus, oviduct, and ovaries were present on the submitted slide. In the uterus, frequent glands were dilated and epithelium was flattened. Glands were usually round, and moderately densely packed with low columnar to cuboidal epithelium. Glands often contained eosinophilic flocculent amorphous contents and rare sloughed epithelial cells. Scattered aggregates of lymphocytes and plasma cells expanded the periglandular superficial endometrium. Some arterioles in the endometrium and myometrium had increased perivascular hyaline material expending the adjacent adventitia.

The ovarian cortices were markedly expanded by large cysts lined by multiple layers of columnar cells (follicular cells), with some reduced to a single layer over much of the surface (pressure atrophy), and filled with wispy eosinophilic material. Occasional rafts of foamy granulosa cells were present in the antrum. In the adjacent cortex, there were multiple primordial, primary, and secondary follicles, with many compressed, distorted, or collapsed oocytes with a variable number of poorly organized follicular cells. In some, there is extensive mineralization of the atretic follicles.

MORPHOLOGICAL/ETIOLOGICAL DIAGNOSIS:

Uterus: Moderate cystic endometrial hyperplasia

Ovaries: Multiple follicular cysts; multiple atretic follicles with mineralization

DISCUSSION:

Cystic endometrial hyperplasia (CEH) is a common lesion seen in many species. However, the pathogenesis of this lesion is likely different across species. Carnivores typically have CEH associated with the long period of diestrus, in which progesterone-secreting corpora lutea dominate. In other species, often those with epitheliochorial placentation, estrogen will drive CEH and can be associated with follicular cysts, estrogen-secreting tumors, or ingestion of estrogenic plants.² In this case, an aged lemur has multiple follicular cysts in both ovaries, likely secreting estrogen and subsequently leading to endometrial hyperplasia. Based on the other degenerative changes in the ovary and the lemur's age (near its expected lifespan), the formation of these cysts is likely associated with aging.¹ This should be distinguished from Polycystic Ovarian Syndrome (PCOS) in women, which can be seen at any time during reproductive life and is associated with hyperandrogenism, not estrogen.

In a study currently underway (Moresco, Agnew; preliminary data), cystic endometrial hyperplasia is common in captive lemurs, as is follicular atresia. Endometrial polyps, leiomyoma, polypoid adenocarcinoma, hydrometra, and endometrial arteriosclerosis and vascular hyaline change. Other common lesions are endometritis, adenomyosis, cervical cysts, cervicitis, and cystic rete ovarii. Data suggests that increasing number of years without reproduction (days since last pregnancy) is associated with a higher risk of CEH. In addition, progestin contraceptives appear to have a different effect on CEH, depending on the species: if data from all species is combined, there is no effect of contraception on CEH;

however, in ring-tailed lemurs, contraception seems to be protective, while in ruffed lemurs, contraception seems to be associated with increased risk of CEH. Contraception is associated with a higher risk of hydrometra, particularly if there is intermittent exposure. Adenomyosis is also associated with CEH, but there is no effect of contraception. The data also supports a continuum from CEH and adenomyosis to polyps.

Neoplasms described in the lemur ovary or uterus are vulvar squamous cell carcinoma, leiomyoma, endometrial carcinoma, granulosa cells tumor, and dysgerminoma; however, more detailed descriptions of reproduction and reproductive pathology in prosimians are lacking.³

REFERENCES:

1. Baumhofer, E. 2017. "Lemur catta" (On-line), Animal Diversity Web. Accessed October 02, 2023 at https://animaldiversity.org/accounts/Lemur_catta/
2. King BF. Development and structure of the placenta and fetal membranes of nonhuman primates. *J Exp Zool.* 1993 Sep 1;266(6):528-40.
3. Remick AK, Van Wettere AJ, Williams CV. Neoplasia in prosimians: case series from a captive prosimian population and literature review. *Vet Pathol.* 2009 Jul;46(4):746-72.

Acknowledgments:

We thank the many veterinarians and zoos that contribute reproductive tracts to the AZA Reproductive Health Surveillance Program (www.stlzoo.org/RHSP). We also appreciate the professionalism and quality of the work provided by the MSU Investigative Histopathology Laboratory.

MICHIGAN STATE
UNIVERSITY

Case 9

Lemur SP14-6507

CONTRIBUTOR(S)/ INSTITUTION:

Dalen Agnew, DVM, PhD, Dipl ACVP¹

¹*Michigan State University College of Veterinary Medicine, East Lansing, MI,
48824, USA*

SIGNALMENT:

14-year-old male Ring-tailed Lemur (*Lemur catta*).

HISTORY:

This adult male ringtail lemur was found dead with no prior signs.

GROSS FINDINGS:

Hydrothorax was noted and the urinary bladder was adhered to the abdominal wall. An unidentified bilobed tubular organ was noted at the base of the urinary bladder and there was concern that this might be a uterine remnant, an abnormality of sexual differentiation.



**COLLEGE OF
VETERINARY
MEDICINE**

Department of
**Pathobiology
& Diagnostic
Investigation**

Michigan State University
Veterinary Medical Center
784 Wilson Road
Rm. D208
East Lansing, MI
48824

PH:517-432-4685
www.pathobiology.msu.edu

HISTOPATHOLOGIC AND CLINICAL PATHOLOGY FINDINGS:

Sections of the grossly unknown tubular structures were identified as seminal vesicles and associated prostate. On one side, the seminal vesicles were obliterated by neutrophils, macrophages, and fewer lymphocytes and plasma cells which extend to the wall to the serosal surface. The duct leading from the vesicular gland also contains abundant neutrophils. Scattered Gram negative rod bacteria are present in the intraluminal exudate. The adjacent prostate gland was occasionally expanded by nodular and more scattered lymphocytes and plasma cells with rare neutrophils. Similarly, the urethral mucosa was infiltrated multifocally with lymphocytes, plasma cells, and occasional neutrophils and macrophages.

Also examined were sections of kidney, stomach, spleen, colon, small intestine, pancreas, adrenal gland, liver, lung, testicle, epididymis, gall bladder, heart, trachea, urinary bladder, esophagus skeletal muscle, and lymph nodes.

In the kidney, there was a solitary, lymphocytic nodule in the cortex and abundant pelvic hemorrhage. The spleen and pancreas had granulomas within the attached mesentery with refractile material. The liver had multifocal lymphoplasmacytic nodules often associated with macrophages randomly scattered in the parenchyma. In these areas, there were some vesicular nuclei, with peripheralization of the chromatin. The lung was diffusely consolidated, with thickened alveolar walls and abundant interstitial and intraluminal hemorrhage. There was a marked increase in the number of circulating neutrophils, lymphocytes and plasma cells, and monocytes, with numerous interstitial mononuclear cells.

The testicle had scant spermatogenesis, shrunken seminiferous tubules with wrinkled basement membranes and frequent multinucleated giant cells. The epididymis lacks any spermatocytes and there are scattered foci of lymphocytes, plasma cells, macrophages, and some neutrophils adherent to the outer surface of the tunic. The urinary bladder has multiple lymphoplasmacytic nodules within the wall, often with germinal centers.

MORPHOLOGICAL/ETIOLOGICAL DIAGNOSIS:

Seminal vesicles: Severe transmural suppurative seminal vesiculitis

Urethra: Mild chronic urethritis

Prostate gland: Mild chronic prostatitis

Additional diagnoses:

Peritoneal cavity: Mild multifocal chronic peritonitis

Lung: Moderate interstitial pneumonia

Liver: Mild multifocal chronic hepatitis

Testicle: Moderate degeneration with hypopermia

DISCUSSION:

The likely cause of death in this lemur was the severe transmural seminal vesiculitis leading to peritonitis and sepsis. Ascending infections of accessory glands are the

most common cause of this lesion in other species, and *E. coli* would be a likely pathogen of interest (unfortunately, cultures were not done on fresh tissue).⁶ The changes in the liver are likely due to longterm inflammatory insults with a superimposed recent sepsis - the nuclear changes are interpreted as degenerative in nature and not likely viral. While cause and effect are not clear in this case, the vesiculitis was likely linked to testicular degeneration and infertility. The lack of hemosiderosis in this animal is unusual in a lemur of this age.

Seminal vesiculitis is not commonly reported in animals, though it is more common in men.^{6,7} Four cases, (3 in baboons and 1 in a macaque) were reported in a primate center survey.⁵ A single report of a case in a ring-tailed lemur was similar to this case, but was identified antemortem via ultrasonography during a routine physical examination.⁴ The lemur in this report also had no clinical signs and only mildly abnormal biochemistry findings at the time of presentation despite the affected vesicular gland being four times the size of the normal contralateral gland. It was treated surgically with a successful outcome. Unfortunately, inflammation was not histologically confirmed in that case. Obstruction and dilation with inspissated coagulum would be another differential.

Like rodents, lemurs have prominent seminal vesicles which contribute a substantial portion of the late ejaculate, creating the vaginal or copulatory plug.¹ This is presumed to have evolved in the context of sperm competition in the presence of polyandry. In both natural and assisted breeding, copulatory plugs can obstruct the male lemur urethra and lead to a life-threatening condition.² Risk factors in any species have not been well-documented, but seminal vesiculitis has been associated with inflammation of other accessory sex glands and in humans, with possible abnormal pattern recognition receptor signalling and expression of semenogelin I.³

REFERENCES:

1. Brun B, Cranz C, Clavert A, Rumpler Y. A safe technique for collecting semen from *Lemur fulvus mayottensis*. *Folia Primatol (Basel)*. 1987;49:48-51.
2. Chatfield JA, Chatfield JJ, Chatfield JA. Urethral obstruction with a copulatory plug following natural breeding in a ruffed lemur, *Varecia rubra*. *J Med Primatol*. 2014 Apr;43(2):115-7.
3. Gong M, Wang F, Liu W, Chen R, Wu H, Zhang W, Yu X, Han R, Liu A, Chen Y, Han D. Pattern recognition receptor-mediated innate immune responses in seminal vesicle epithelial cell and their impacts on cellular function. *Biol Reprod*. 2019 Oct 25;101(4):733-747.
4. Hayhurst SE, Engel JD, Walsh T, Gordon S, Murray S, Boedeker N. What is your diagnosis? Seminal vesicle disease. *J Am Vet Med Assoc*. 2015;246:839-41.
5. Kirejczyk S, Pinelli C, Gonzalez O, Kumar S, Dick E Jr, Gumber S. Urogenital Lesions in Nonhuman Primates at 2 National Primate Research Centers. *Vet Pathol*. 2021 Jan;58(1):147-160.

6. Pozor M. Seminal Vesiculitis. In: Orsini JA, Genager NS, de Lahunta A, ed. *Comparative Anatomy*. 1st ed. London, UK: Academic Press; 2022:825-833.
7. Zhang P, Wang XL, Yang ZH, Su XJ, Wang XH. A novel rat model of seminal vesiculitis. *Asian J Androl*. 2019;21:360-364.

Acknowledgments: We thank the veterinary and keeper staff at Gladys Porter Zoo for their care of this lemur and providing case history. We also thank the dedicated histopathology staff at the Michigan State University Veterinary Diagnostic Laboratory.



Sarah Beck, DVM, PhD, DACVP
Charles River Laboratories

Signalment: 5-year-old male *Cynomolgus* macaque

History:

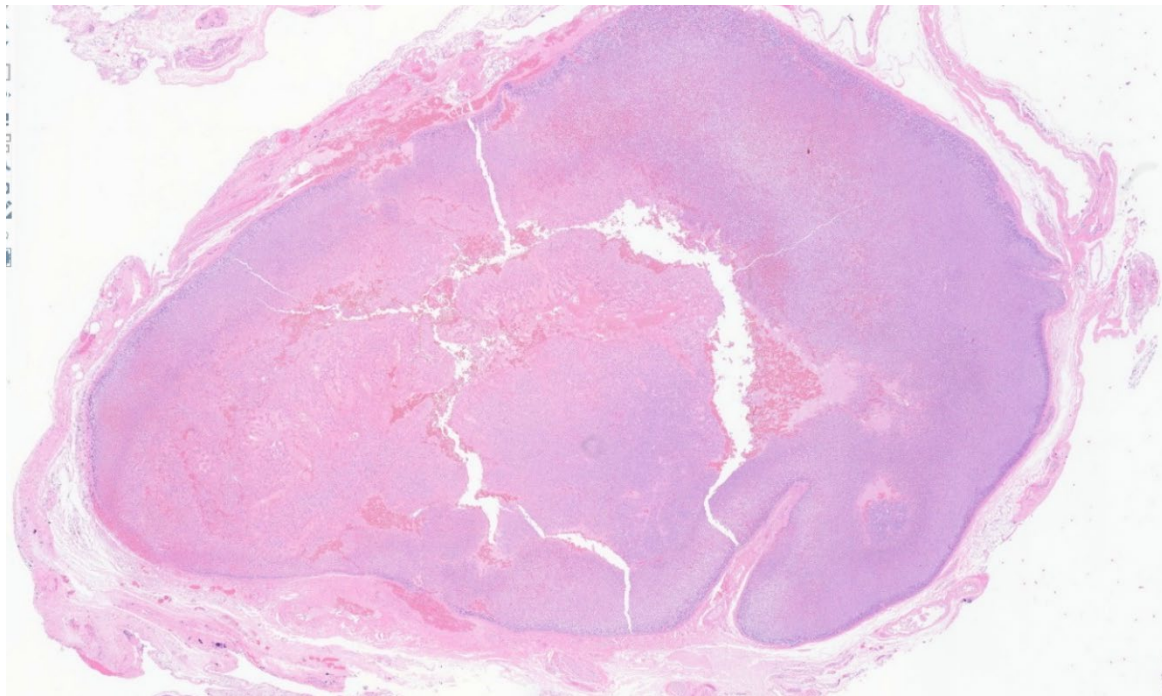
A male cynomolgus macaque that had been in the facility colony since June 2021 had an initial observation of decreased activity in July 2023 and was examined by the veterinary staff. In addition to decreased activity, the monkey had hunched posture, a slow and slightly ataxic gate, drooping of the left side of face, no blink response in the left eye, and mild full body tremors. In the afternoon of the same day, the monkey was tilted to the left with drooping of the left lip, weak on the left side and ataxic. There was a 102 °F body temperature and dried discharge was observed in the left ear. The monkey was started on amoxicillin/clavulanate and meloxicam. The following morning, the monkey was laying on the cage floor with tremoring, shivering, nystagmus, more drainage from the left ear, and a body temperature of 97.3 °F. Given the progression of clinical signs, the monkey was euthanized and sent to necropsy.

Gross Findings:

A unilateral adrenal 'mass' was observed that was firm, mottled and measured 20 x 10 x 5 mm. Given the clinical signs and gross observation, the ear, brain, and adrenal 'mass' were collected, fixed in 10% neutral buffered formalin and processed to slide.

Microscopic Findings:

Adrenal gland: The adrenal gland 'mass' was identified as adrenal gland microscopically. The cortex, medulla, and capsule were expanded by large numbers of erythrocytes (hemorrhage and congestion) and proteinaceous fluid. Occasionally, small venules contained basophilic aggregates that were consistent with bacteria. There was multifocal and focally extensive necrosis of the cortex and medulla characterized by disorganized, pale and eosinophilic cells with occasional pyknosis and inflammatory cells in the capillaries.



Diagnosis:

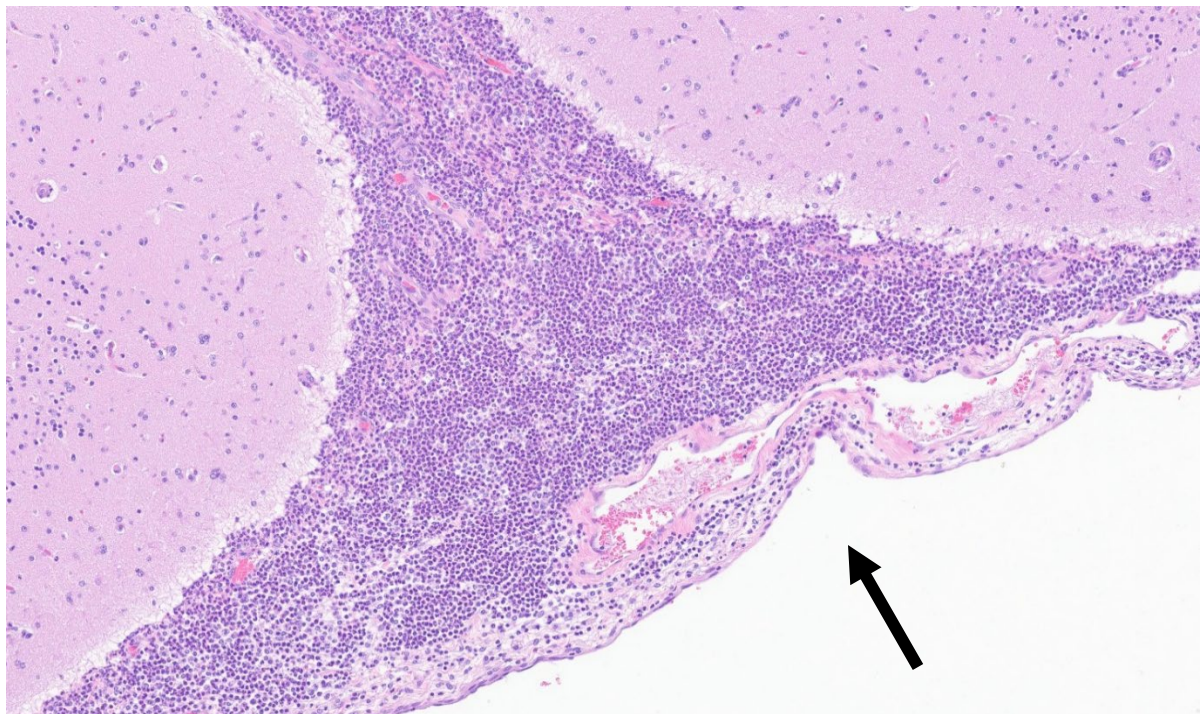
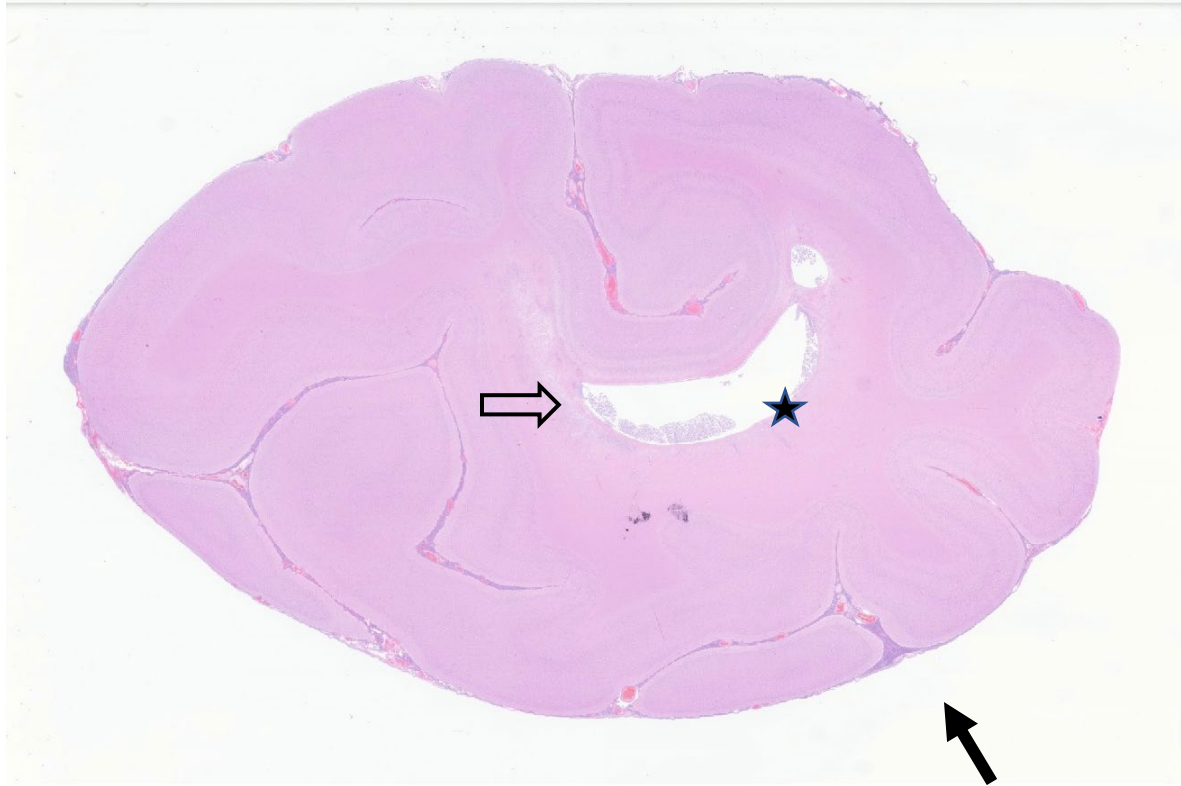
Adrenal gland – moderate hemorrhage and congestion, capsule, cortex, and medulla with intravascular bacterial colonies

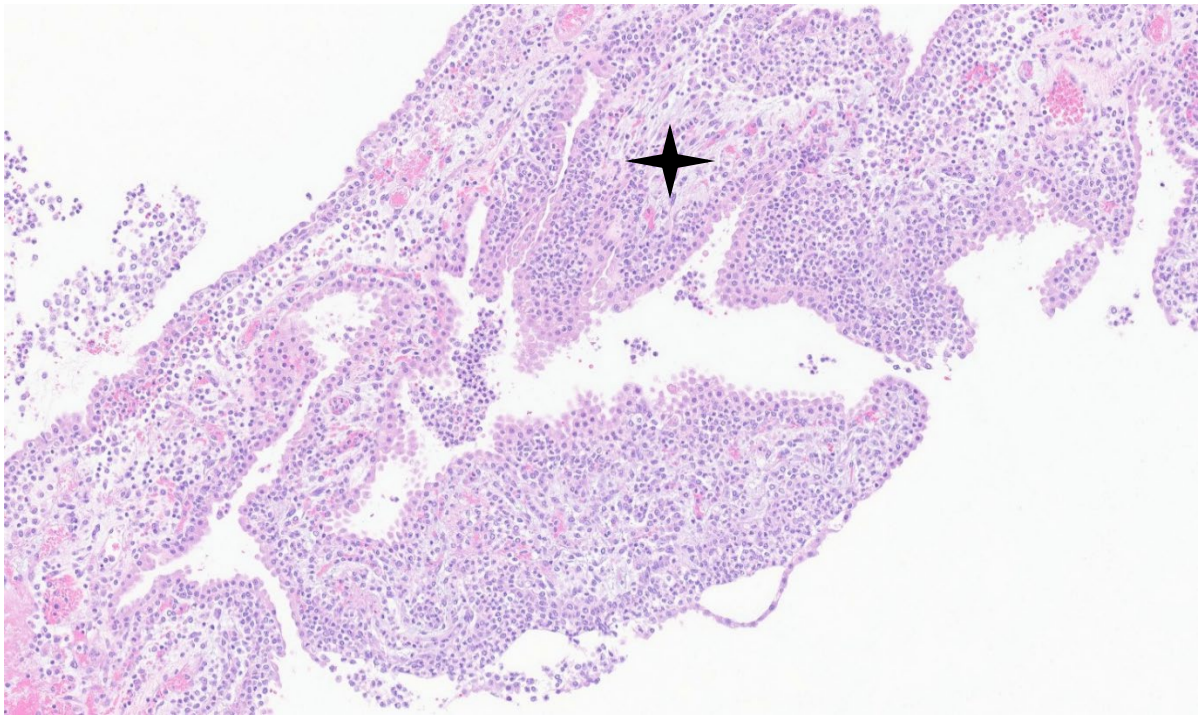
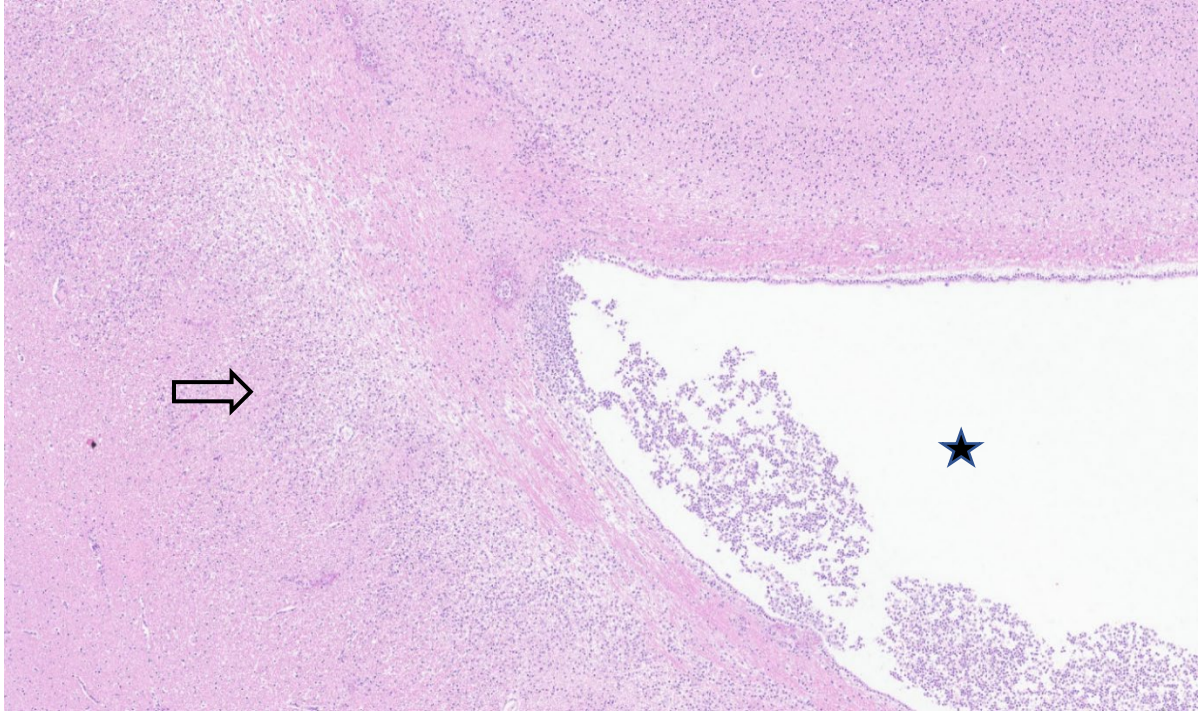
Adrenal gland – moderate, regionally extensive necrosis, cortex and medulla

Discussion:

Adrenal gland changes were consistent with those described in Waterhouse-Friderichsen syndrome (WFS).¹ There are many etiologies associated with WFS and include bacterial meningitis, bacterial sepsis, or systemic viral infections, among others. A specific pathogenesis for WFS is not known but may be associated with changes in adrenal vascular pressure, vascular damage from bacterial toxins, or coagulopathy associated with disseminated intravascular coagulation.

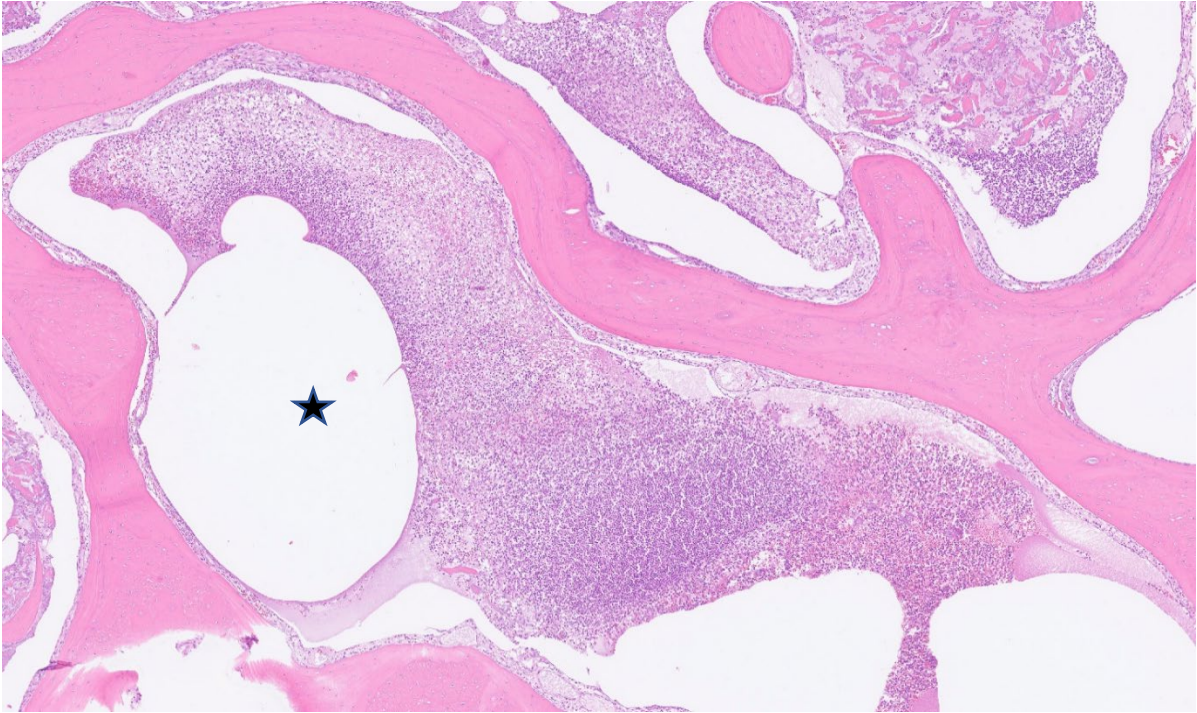
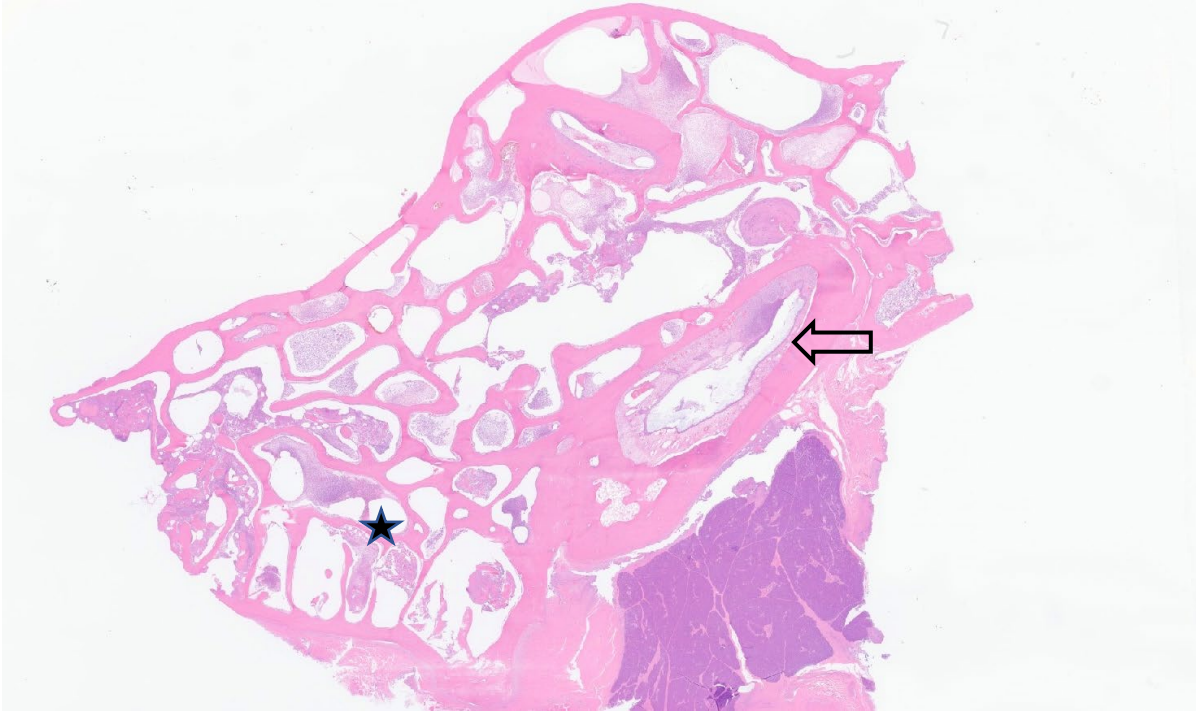
In this cynomolgus monkey, there was marked suppurative meningitis (solid arrow), ventriculitis (five-point star), and choroid plexitis (four-point star) in all areas of the brain with necrosis and inflammation of neuropil (open arrow) adjacent to the ventricles. Waterhouse Friderichsen syndrome has also been reported in a cynomolgus monkey associated with Staphylococcal meningitis.²

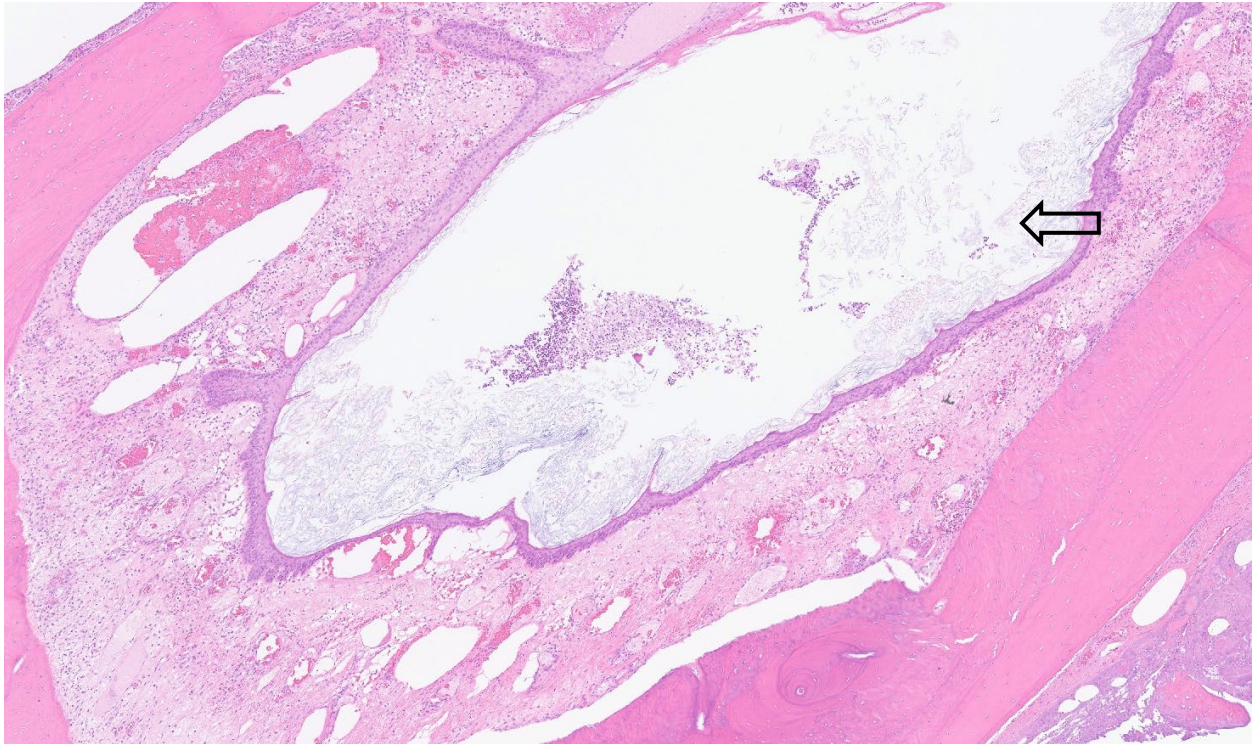




The most likely source for the suppurative inflammation in the brain was the ear given the discharge that was observed along with the neurologic signs. The mastoid process of the temporal bone is part of the middle ear in monkeys³ and was evaluated in this case. The inflammation in the mastoid process was similar to that observed in the brain (with more fibrin and possible bacteria admixed with the cell debris) and was located in the mastoid air cells

(five-point star) and in the portion of the external ear canal (open arrow) present in the photomicrograph.





References:

1. Karki BR, Sedhai YR, Bokhari SRA. Waterhouse-Friderichsen Syndrome. [Updated 2023 Jun 26]. In: StatPearls [Internet]. Treasure Island (FL): StatPearls Publishing; 2023 Jan-. Available from: <https://www.ncbi.nlm.nih.gov/books/NBK551510/>
2. Lin Z, Zhang L, Zhang D, et al. A case report of spontaneous staphylococcal meningitis in a cynomolgus monkey. *J Med Primatol*. 2018;47(2):132-135.
3. Wysocki J. Topographical anatomy and morphometry of the temporal bone of the macaque. *Folia Morphol (Warsz)*. 2009;68(1):13-22.